

Microwave Noise of Si/Si_{0.6}Ge_{0.4} Heterojunction Bipolar Transistors

S. Mohammadi¹⁾, L.-H. Lu¹⁾, Z. Ma¹⁾, L.P.B. Katchi¹⁾, P.K. Bhattacharya¹⁾, G.E. Ponchak²⁾
and E.T. Croke³⁾

¹⁾Department of Electrical Engineering, The University of Michigan, Ann Arbor, MI 48109-2122, USA. ²⁾NASA Lewis Research Center, Cleveland, OH 44135, USA. ³⁾Hughes Research Laboratory, Malibu, CA 90265, USA

Abstract¹- The microwave noise of Si/SiGe HBTs was characterized and modeled using a high-frequency T-equivalent noise circuit model. A 6 finger 2×15 μm² HBT showed a minimum noise figure of 2.26dB with an associated gain of 12.7dB, measured at 8 GHz under I_C=14mA and V_{CE}=3V bias condition. Bias, frequency and HBT geometry dependent noise measurements were also performed. It was found that the 6 finger 2×15 μm² HBT has the best noise performance among the characterized devices. Moreover, it was revealed that minimum noise figure reaches a minimum at a medium collector current. Finally, a simple all physical high-frequency T-equivalent noise model was extracted from the measured S-parameters and noise data and was used for the study of noise dependence on different HBT equivalent circuit parameters.

Introduction

Microwave monolithic integrated circuits based on Si technology (Si MMICs) have recently received great attention due to their lower cost compared to III-V devices. The integration of high-frequency high-performance Si/SiGe HBTs with CMOS circuitry has permitted the realization of complex systems such as RF receivers using a single Si substrate. The noise figure of the receiver system is dominated in this case by the transistor noise performance. A 6.25GHz 2.2dB noise figure, low noise amplifier based on Si/SiGe HBT with low Ge concentration has been reported by IBM [1], while the noise performance of Si/SiGe HBTs with high Ge concentration at such high frequencies has not been reported.

1. Si/SiGe HBT Technology

Si/SiGe HBTs with high Ge concentration in the base (Ge mole fraction ≈ 0.3-0.4) were fabricated on high-resistivity silicon substrate using a self-aligned technology. Although this technology is currently optimized for high-power devices, it proved to show good microwave noise performance. The technology consists of several RIE dry and KOH wet selective etching, contact metal evaporation, and lift-off steps. A PECVD SiO₂ layer is used for passivation and inter-metal dielectric. The HBT layer structure is shown in Table. 1 and details of the fabrication process are reported by the authors elsewhere [2]. A 6 finger 2×15 μm² HBT achieved f_T of 18GHz and f_{max} of 34GHz under I_C=14mA and V_{CE}=3V bias condition.

N+ Si	emitter contact	2×10 ¹⁹ cm ⁻³	200 nm
N Si	emitter	2×10 ¹⁸ cm ⁻³	100 nm
I Si _{0.6} Ge _{0.4}	spacer	NID	5 nm
P+ Si _{0.6} Ge _{0.4}	base	2×10 ¹⁹ cm ⁻³	20 nm
I Si _{0.6} Ge _{0.4}	spacer	NID	5 nm
n- Si	collector	5×10 ¹⁵ cm ⁻³	300 nm
N+ Si	Sub-collector	1×10 ¹⁹ cm ⁻³	1500 nm
p- Si	substrate	1×10 ¹² cm ⁻³	540 μm

Table 1: Layer design of Si/SiGe HBT.

¹ Work supported by NASA-JPL under contract 961356.

2. Microwave Noise Characterization

The high-frequency noise performance of Si/SiGe HBTs was experimentally investigated using on-wafer noise characterization system shown in Figure 1. A computer-controlled mechanical tuner is connected to the input of the device under test to provide different source impedances necessary for high-frequency noise evaluation. The set-up allows accurate high-frequency noise measurement through the possibility of in-situ calibration of the system and simultaneously measurement of HBT high-frequency noise and S-parameters. Four noise parameters of the HBT, *i.e.* F_{min} : the minimum noise figure, R_n : noise equivalent resistance and G_{opt} : magnitude and phase of the optimum source reflection coefficient [3] were obtained experimentally by measuring the noise power under at least five different source impedance conditions. Fig. 2 shows such noise characteristics measured for the 4 finger $2 \times 15 \mu m^2$ Si/SiGe HBT at 6GHz. The noise figure and associated gain contours are given here ($F_{min}=2.2\text{dB}$ and $G_A=8.0\text{dB}$) at a bias condition of $I_C=9\text{mA}$ and $V_{CE}=2.5\text{V}$.

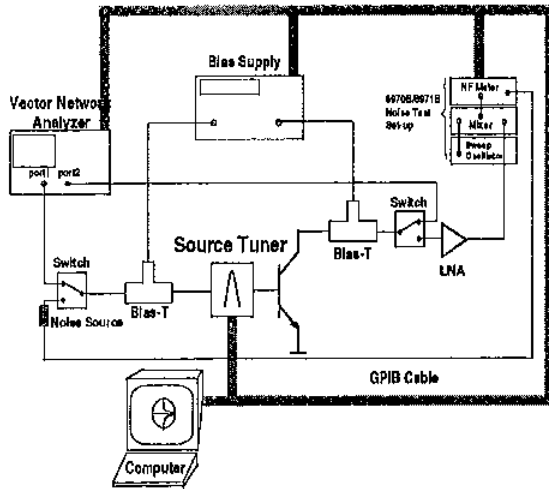


Figure 1: High-frequency noise measurement setup.

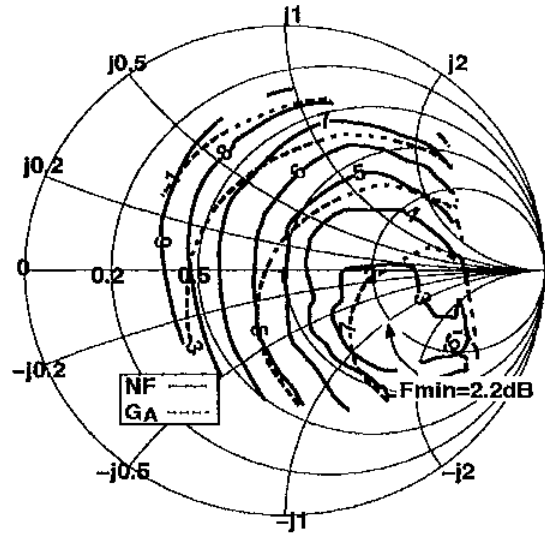


Figure 2 Noise characteristics of 4 finger $2 \times 15 \mu m^2$ Si/SiGe HBT at 6GHz.

Fig.3 shows the measured minimum noise figure (F_{min}) and associated gain (G_A) of Si/SiGe HBTs with different geometry at 8GHz. Each device is biased at $V_{CE}=3\text{V}$ and at an optimum collector current I_C (also shown in the figure) which resulted in smallest F_{min} . The 6 finger $2 \times 15 \mu m^2$ Si/SiGe HBT showed the lowest minimum noise figure of 2.26dB and the highest associated gain of 12.7dB at 8GHz among the characterized devices.

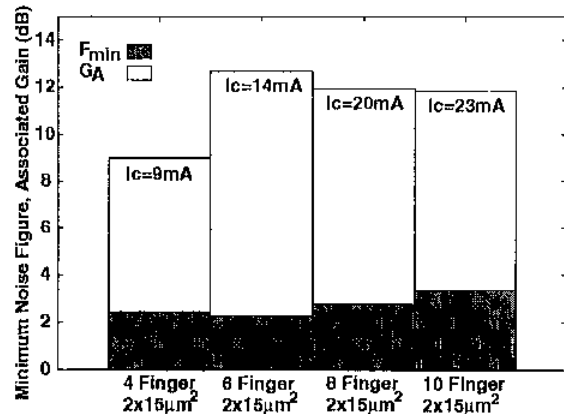


Figure 3: Minimum noise figure and associated gain of HBTs with different geometry at 8GHz in the order of increased HBT area.

3. HBT Noise Modeling

Figure 4 shows the noise equivalent circuit of the HBT used in this work, which is based on a T-equivalent model derived from S-parameter measurements by direct analysis and from noise data. Also shown in the figure are the small-signal parameters of the 6 finger $2 \times 15 \mu\text{m}^2$ Si/SiGe HBT biased at $V_{CE}=3\text{V}$ and $I_C=14\text{mA}$. The ratio of $i_L^2/i_{L,\text{noiseless}}^2$ (i_L : collector short-circuit current, $i_{L,\text{noiseless}}$: collector short-circuit current with a noiseless transistor), which is the noise figure [4] was evaluated analytically using the equivalent circuit of Fig. 4. Next, the four noise parameters were calculated, and the importance of device design on each noise parameter was identified.

Fig. 5 shows the modeled and measured frequency dependence of the minimum noise figure and noise equivalent resistance of the 6 finger $2 \times 15 \mu\text{m}^2$ Si/SiGe HBT biased at $V_{CE}=3\text{V}$ and $I_C=14\text{mA}$ using the noise model of Fig. 4.

$L_c(\text{nH})$	$L_b(\text{nH})$	$L_e(\text{nH})$	$r_b(\Omega)$	$r_e(\Omega)$	$r_{be}(\Omega)$
0.023	0.025	0.02	10.5	1.3	1.6
$\tau_f(\text{ps})$	$C_{bc}(\text{pF})$	$C_{p1}(\text{pF})$	$r_c(\Omega)$	$r_{bx}(\Omega)$	$C_{bx}(\text{pF})$
11	0.15	0.036	11.8	3	0.003

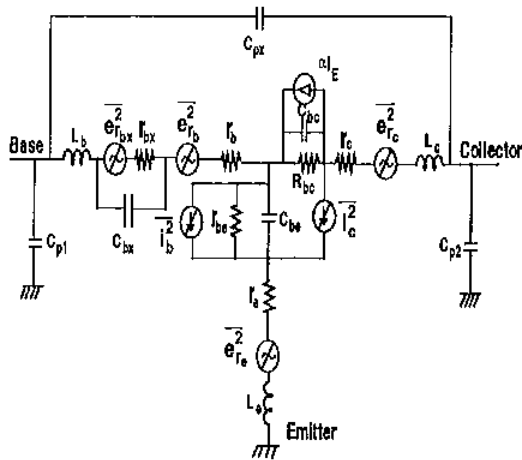


Figure 4: Small-signal high-frequency noise model of Si/SiGe HBT

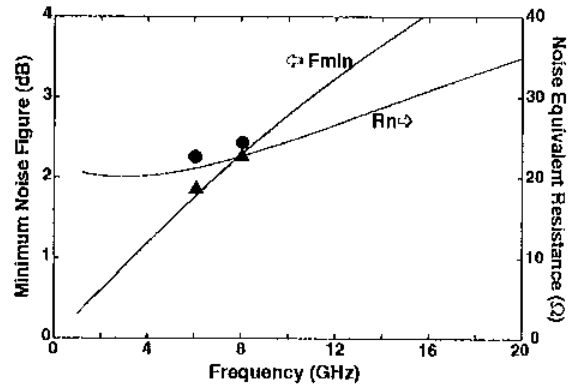


Figure 5: Frequency dependence of minimum noise figure and noise equivalent resistance of the 6 finger $2 \times 15 \mu\text{m}^2$ Si/SiGe HBT. The measured values at 6 and 8GHz are also shown.

The important factors determining the noise and gain characteristics of the HBT were found to be the base series resistance (r_b), the base-emitter junction incremental resistance (r_{be}), the HBT forward transit time (τ_f) and the collector current (I_C). Other parameters including the junction capacitances in the HBT noise model of Fig. 4 were found to have small impact on the noise performance of the Si/SiGe HBTs analyzed in this work. This is due to the fact that the noise performance of these devices is limited by the base series resistance thermal noise and the collector current shot noise components. The forward transit time (τ_f) appears to limit the device gain and therefore noise characteristics at high frequencies.

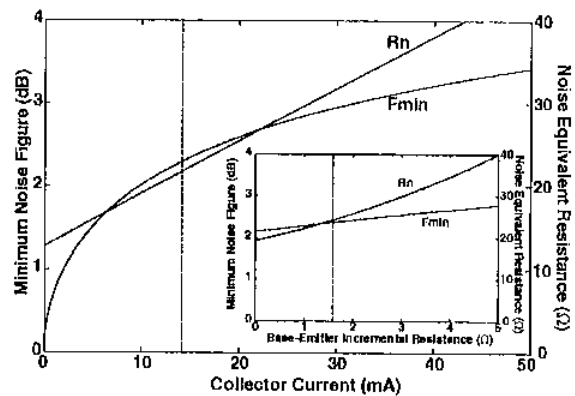


Figure 6: Minimum noise figure and noise equivalent resistance of Si/SiGe HBT as a function of the collector current shot noise and base-emitter incremental resistance.

Fig. 6 shows the variation in the HBT minimum noise figure and noise equivalent resistance with the collector current shot noise. It is worth noting that in the simulation of Fig. 6, only the shot noise component in the small-signal noise model of Fig. 4 is varied. In practice, when the collector current is changed, the base-emitter incremental resistance (r_{be}) and also the device forward transit time (τ_f) vary with collector current. Therefore the dependence of noise parameters on r_{be} and τ_f needs to be clarified. Shown in the inset of Fig. 6 is the dependence of F_{min} and R_n on r_{be} . As the figure indicates, minimum noise figure increases with increased collector current shot noise (higher I_C), but decreases for decreased r_{be} (higher I_C). The dashed lines in Fig 6 indicate the nominal parameter values for the 6 finger $2 \times 15 \mu m^2$ Si/SiGe HBT.

Fig. 7 shows the variation of the minimum noise figure and noise equivalent resistance on the HBT forward transit time (τ_f). As shown in the figure, the forward transit time significantly impacts the minimum noise figure, but has a small effect on the noise equivalent resistance. The dashed line indicates the forward transit time of 11psec which was extracted for the 6 finger $2 \times 15 \mu m^2$ Si/SiGe HBT under $V_{CE}=3V$ and $I_C=14mA$ bias condition.

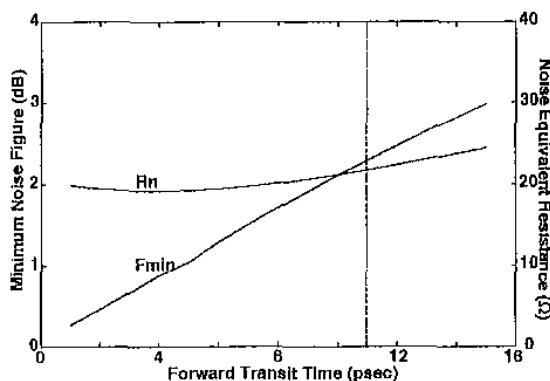


Figure 7: Dependence of minimum noise figure and noise equivalent resistance on the forward transit time of the HBT.

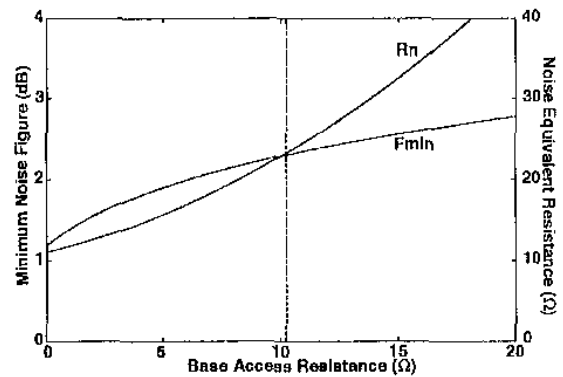


Figure 8: Dependence of minimum noise figure and noise equivalent resistance on the HBT base access resistance.

Finally, Fig. 8 shows the variation of the minimum noise figure and noise equivalent resistance of the 6 finger $2 \times 15 \mu m^2$ Si/SiGe HBT vs. the base access resistance (nominal value 10.5Ω). Because the base access resistance in these devices is not yet optimized, both F_{min} and R_n show significant dependence on this parasitic resistance.

Overall, this work presents the preliminary results of high-frequency noise of Si/SiGe HBTs with high Ge concentration in the base, with good noise performance ($F_{min}=2.26dB$ at 8GHz). Based on the model developed in this work, further improvement in the noise performance can be achieved by optimizing the HBT layer structure as well as device geometry. This work is in progress and the results forthcoming from the effort on devices and LNAs will be presented.

4. References

- [1] H. Ainspan *et al.*, "6.25GHz low DC power low-noise amplifier in SiGe," Proceedings of the Custom Integrated Circuits Conference, pp. 177-180, 1997.
- [2] J.-S. Rieh *et al.*, "X- and Ku-band amplifiers based on Si/SiGe HBT's and micromachined lumped components," IEEE Trans. On Microwave Theory and Techniques, v. 46 n 5, pp. 685-694, 1998.
- [3] H. Fukui, "Optimal noise figure of microwave GaAs MESFET's," IEEE Trans. on Electron Devices, v. 26 n7, pp. 1032-1037, 1979.
- [4] R.J. Hawkins, "Limitations of Nielsen's and related noise equations applied to microwave bipolar transistors, and a new expression for the frequency and current dependent noise figure," Solid-State Electronics, v. 20 n. 3, pp. 191-196, 1977.